Graphical and algebraic synthesis for PWM methods

AUTHORS

S. L. CAPITANEANU, B. de FORNEL, M. FADEL, J. FAUCHER, A. ALMEIDA

EPE Journal Vol 11 N°3 – Aout 2001

ENSEEIHT/INP TOULOUSE

Laboratoire d'Electrotechnique et d'Electronique Industrielle

15-mars-04

Graphical and algebraic synthesis for PWM methods

S. L. Capitaneanu – Laboratoire d'Electrotechnique et d'Electronique Industrielle, Toulouse, France
B. de Fornel – Laboratoire d'Electrotechnique et d'Electronique Industrielle, Toulouse, France
M. Fadel – Laboratoire d'Electrotechnique et d'Electronique Industrielle, Toulouse, France
J. Faucher – Laboratoire d'Electrotechnique et d'Electronique Industrielle, Toulouse, France
A. Almeida – Schneider Toshiba Inverter Europe, Pacy sur Eure, France

Schneider Toshiba Inverter Europe – LEEI collaboration

ABSTRACT

The article proposes an algebraic synthesis for PWM methods, which is based on a graphical representation of the 2 levels VSI (Voltage Source Inverter). This theory can be the starting point for every PWM method representation.
In order to understand the historical evolution of the PWM methods the authors propose two classification groups of the main PWM techniques. The main classification is based on the movement of the neutral point (zero-voltage V_{N0} evolution). The details of PWM methods presented here are also seen from the graphical representation perspective.
The equivalence between the well-known SVM (Space Vector Modulation) practically DDT realized (Direct Digital Technique) and the three-phase PWM with a carrier based industrial realization is shown. The principles of the three-phase PWM and the 3rd harmonic injection PWM (THIPWM4, THIPWM6) are compared the same as the DPWM (Discontinuous PWM) methods.
These classifications and equivalences between different techniques show that the number of contemporary used PWM principles can be reduced.
The general complex space representation and the classifications proposed here are simple to comprehension educational tools and they simply the way towards practical implementation.

Keywords: PWM, graphical synthesis, DPWM, SVM, three-phase PWM, zero-voltage

GLOSSARY

a_i, i=1,2,3: inverter duty cycles
α_i, i=0,…,7: inverter voltages application times
Ci, i=1,…,6: inverter IGBTs
E=bus voltage
f_m: frequency of the reference wave (modulation wave)
f_{PWM}: PWM switching frequency
m_a: modulation amplitude
m_i : modulation index
Sci, i=1,2,3 : inverter orders for the 6 switches
T_e: sampling period
Ti[k], i=1,2,3: pulse width at k sampling instant
V_{i0}, i=1,2,3: inverter line voltage
V_{iN}, i=1,2,3: motor line voltage from supplying point of view (*fig.1*)
V_{iref}, i=1,2,3: inverter reference voltages
V_{medium}: medium voltage as in *fig.23*
V_{N0}: zero-voltage or zero-sequence signal (*fig.1*)
V_{PWM}: fundamental of the reference voltage when using PWM method
V_{ref}: inverter reference voltage in complex representation
$V_{six\text{-}step}$: fundamental of reference voltage when using six-step wave
V_s: motor voltage in complex representation

DDT: direct digital technique (for PWM implantation) [2], [7]
CPWM: continuous PWM
DPWM: discontinuous PWM [10], [11], [15], [16], [17], [18]
DPWM0, 1, 2, MLVPWM, DPWMMIN, DPWMMAX: different discontinuous PWM techniques
GDPWM: generalised discontinuous PWM [10], [11]
RPWM: random frequency PWM [24]
SPWM: sinusoidal PWM [1]
SVM: space vector modulation [2], [7]
THIPWM4 or **6**: PWM with 3rd harmonic injection [3], [6]
Three-phase PWM: PWM with V_{medium} injection with modulation wave/triangular carrier implantation [4], [5], [23]
VSI: Voltage Source Inverter

INTRODUCTION

The **PWM** (Pulse Width Modulation, sometimes used with an older denomination: Pulse-Duration Modulation) is a technique used for energy conversion with bases in telecommunications domain (signal processing). The **modulation** is a process of varying a characteristic of a carrier in accordance with a piece of information (data). In Power Electronics the information is the magnitude, the frequency and the phase of voltage or current. The PWM plays with the width of (voltage or current) pulses in order to output the average reference signal.
The VSIs are static DC⇔AC converters with application in AC drives, UPS (Uninterrupted Power Supply) and interface utility. The PWM technique varies the width of the pulses obtained by chopping a continuous voltage (bus voltage E). The 2 levels inverter as well as the notations used afterwards are represented in *fig.1*.

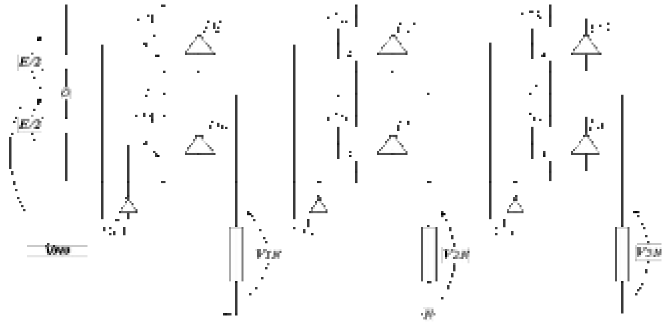

Fig.1 PWM-VSI connected to a general load.

Let the IGBTs be C1, C2…C6 and the on/off orders of the 6 switches be Sc1, Sc2, …, Sc6 (positive logic) :

$$Sci=\begin{cases}1, Ci=on\\0, Ci=off\end{cases}, \ (\forall)\ i=\overline{1,6} \qquad (eq.1)$$

We note that when Sc1 is 1 Sc4 can't be 1, but when Sc1 is 0 Sc4 can be 0. The same happens with Sc2/Sc5 and Sc3/Sc6. This is explained by the fact that we can't short-circuit the source (Sc1=Sc4=1), but we can put Sc1=Sc4=0. All existing PWM methods use Sc4, Sc5, Sc6 orders complementarily to Sc1 and, respectively, Sc2, Sc3, so that we can give up studying Sc4, Sc5, Sc6 when Sc1, Sc2, Sc3 well defined.

We will present the 8 possibilities of switching cases and the entire theory of the inverter's complex representation in the third section. Historically, the orders Sc1, Sc2, Sc3 were firstly obtained by the comparison of a triangular carrier wave with a reference modulation wave that was sinusoidal [1]. The frequency of the carrier must be much greater than the frequency of the modulation wave in order to obtain good performances for the output wave (modulated signal).

We will concentrate the study on the most common application of the PWM-VSI: the AC motor drive (*fig.2*).

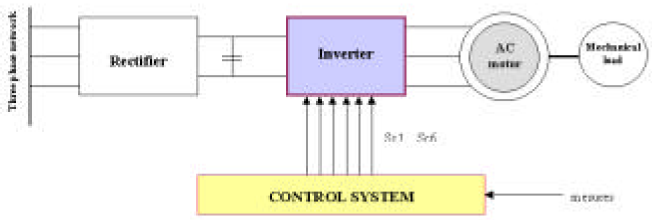

Fig.2 AC drive – AC motor sytem

We will firstly present the original PWM technique (**SPWM**) and its digital successor (**regular PWM**), as these methods were the first steps of the Pulse Width Modulations in Power Electronics. Then we will propose a simple graphical representation for the PWM methods that is based on an algebraic model of the 2 levels VSI: **the "complex cube" representation**. We will interpret the most known PWM techniques in the "complex cube" perspective. This interpretation will be built on 2 group classifications in order to emphasize the main common characteristics of PWM principles. We will prove afterwards some equivalence between PWM methods as well as the fact that a few PWM techniques are less useful compared to some contemporary ones that sometimes includes the older principles.

Because of the limited space, this study will not take into account the current controlled PWM as well as a few less known PWM techniques.

REVIEW OF THE BASIC PWM TYPES

1) The principle of Schönung and Stemmler [1] used under **SPWM (Sinusoidal PWM)** name is presented in *fig*.3. The reference voltage, which is the voltage imposed by the user, is not the expected **motor line voltage**, but the **inverter line voltage** (*fig.1*). The relations between the motor line voltage and the inverter line voltage are developed further.

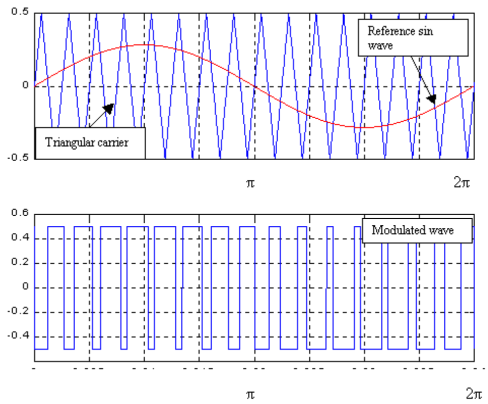

Fig.3 Comparison of modulation wave / triangle carrier and resulting modulated wave (normalised with respect to E)

Every instant the modulated voltage wave is:

$$V_{i0}=\frac{E}{2}\cdot(2\cdot Sc_i-1),\ i=\overline{1,3} \qquad (eq.\ 2)$$

Sci=1 if the modulation wave value is greater or equal to the carrier value and 0 if not.

As we could see in the next section, applying to the inverter a reference voltage that is exactly the expected motor line voltage ($V_{i0}=V_{iref}=V_{iN}$, i=1,2,3) reduces the domain of the linearity of the 2 levels inverter. **The domain of linearity** is the variation interval where the average of the modulated wave evolutes linearly with the modulation wave. The algebraic three-phase PWM method (and also the SVM technique) consists in using the mid-point-to-neutral voltage $\mathbf{V_{NO}}$ (usually called **zero sequence signal**) in the voltage reference. The result is that we can obtain the expected motor voltage applying something different to the inverter ($V_{i0}=V_{iN}+V_{N0}$). This will be detailed in the next section.

The SPWM have got a few different supplementary names function of the triangle carrier:

- **Symmetrical SPWM,** when the triangle carrier was symmetric (*Fig.4a*)
- **Leading edge SPWM,** when the mounting slope is infinite (*Fig 4b*)
- **Trailing edge SPWM,** when the descendant slope is infinite (*Fig 4c*).

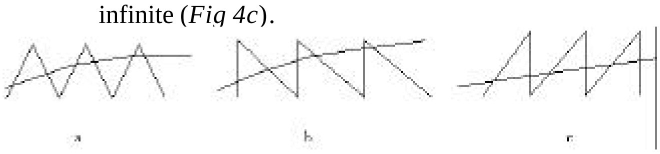

Fig.4 Most common carrier types

In fact the fronts of the carrier constitutes a liberty degree for different PWM methods so that an entire group of PWM types has been formed only by changing the carrier (for example: one of the random PWM [21]).

It was shown [2] that any symmetrical PWM has better results (concerning current ripple) than the asymmetrical PWM, because the frequency that the motor line voltage sees is 2 times greater than the switching frequency $\mathbf{f_{PWM}}$.

There are also two types of SPWM (and generally PWM) function of the position of the carrier reported to the modulation wave:

- **Synchronous SPWM**, when the carrier frequency is a multiple of the sine wave frequency ($f_{PWM}=k*f_m$)
- **Asynchronous SPWM**, when $f_{PWM}\neq k*f_m$

At low carrier frequency the difference between a synchronous and an asynchronous SPWM increases, which introduces sub-harmonics in the spectrum of the modulated wave. With the evolution of power electronics, high-speed switching times are available, so that the carrier frequency is usually high. Anyway, with the apparition of sub-harmonics the amplitude of main harmonics falls and signal degradation may occur.

2) The SPWM has been frequently employed because of its analogical implantation flexibility, but it was difficult to have a digital implementation of the Sinusoidal PWM. The SPWM implies transcendental equations to solve or requests a large number of samples of the sine modulating wave to be stored in a ROM in order to achieve reasonable accuracy. This ended with discovering the **regular PWM** [3]. In the regular PWM the modulation wave is sampled by a zero-order hold so that the value compared to the carrier is constant every sampling period (**T_e**). The average modulated wave value is equal to its constant reference value (*fig.5*).

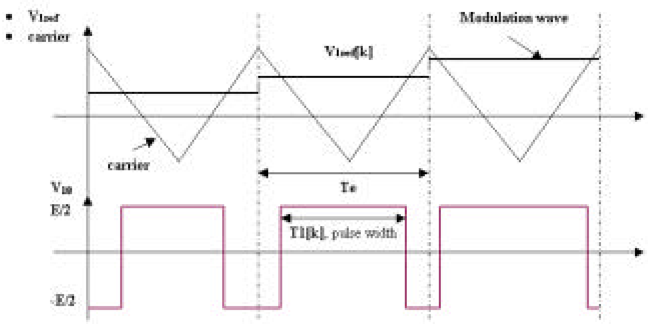

Fig.5 Regular PWM; one phase voltage

$$V_{i\,ref}[k]\cdot T_e = E\cdot Ti[k] - \frac{E}{2}\cdot T_e,\ i=\overline{1,3} \qquad (eq.\ 3)$$

In the *eq. 3* **k** is the sampling instant. It has been shown [20] that the sampling introduces a delay of $T_e/2$ to the output voltage reported to the reference, as well as a gain to every harmonic of the resulting voltage spectrum. For high **f_{PWM}** this becomes insignificant.

A second digital implementation was the regular PWM hold twice a T_e period, every positive or negative top of the triangular carrier. This technique improves the accuracy of the modulated wave. Every edge of the pulse is modulated by a different amount.

One of the biggest inconvenient of PWM techniques is that the spectrum of the motor line voltage is not composed only by the expected sinusoidal, but also by high harmonics at different frequencies.

Many studies have been made in order to manually calculate these harmonics. Nowadays, automatic calculation permits to focus studies not on the calculus, but on the interpretation of it. Taking the case of the regular PWM, we can see from the following results (*table 1*) that the first main harmonics appear at the switching frequency f_{PWM} in the spectrum of the inverter line voltage V_{i0}.

	Frequency $nf_{PWM} \pm qf_m$	*Amplitude*
n odd, q peer	$2kf_{PWM} \pm (2p-1)f_m$	$\frac{\lvert A_{n,q}\rvert}{E} = \frac{4}{np}\left\lvert J_q\left(n\frac{p}{2}m_a\right)\right\rvert$
n peer, q odd	$(2k-1)f_{PWM} \pm 2pf_m$	

Table 1 Amplitude and frequency of regular PWM V_{i0} harmonics.

n, k, p and q are positive numbers, m_a is the modulation amplitude:

$$m_a = \frac{V_{\text{modulation wave}}}{V_{\text{carrier}}} \qquad (eq.\ 4)$$

and J_q is the Bessel function $J_q(z) = \left(\frac{z}{2}\right)^q \sum_{r=0}^{\infty} \frac{(-1)^r}{r!\,(q+r)!}\left(\frac{z}{2}\right)^{2r}$.

The composition of these harmonics (from V_{10}, V_{20}, V_{30} spectra) gives the spectrum of the motor line voltages. The first important harmonics of V_{iN} appear also at $f_{PWM} \pm f_m$ (*fig.6*).

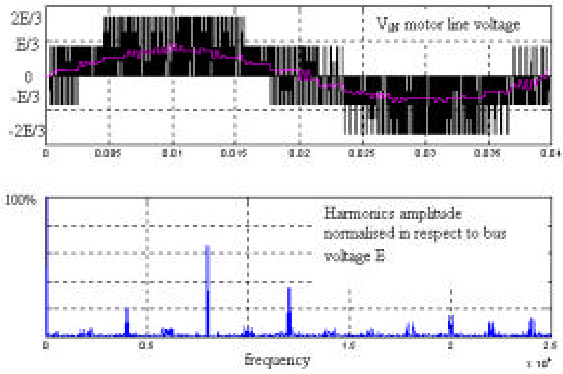

Fig.6 Motor line voltage and its spectrum; simulation for f_{PWM}=4000 Hz, fm=25 Hz $\left(f_{PWM}/f_m = 160\right)$.

SPATIAL COMPLEX REPRESENTATION FOR PWM

The SVM technique (see next section) has introduced not only a modulation technique with high linearity performances and good spectral properties, but also the idea of a complex plane representation of voltage inverters. The **zero-voltage V_{N0}** has opened the way to more PWM types. The idea was a very simple one: **any quantity equally added to each one of the three inverter line voltages V_{i0} gives no result to the motor line voltage V_{iN}.** This quantity creates only a "movement" of V_{NO} when the neutral point is isolated, as in most cases of industrial applications.

If we use the zero-voltage complex representation we must extend the plane complex inverter model to a **3 dimensional** one. Let's introduce the complex plane theory. We will limit the study to the 2 levels VSI.

We must insist on the fact that generally the voltage applied to the inverter is not the expected motor line voltage. This may be possible when the motor neutral point is isolated.

From *eq.2* and *eq. 3* we have:

$$a_i[k] = \frac{1}{2} + \frac{V_{i\,ref}[k]}{E} \qquad (eq.\ 5)$$

if we consider the duty cycle $a_i = \frac{Ti[k]}{T_e}$.

Taking in account that:

$$V_{N0} = \frac{V_{10}+V_{20}+V_{30}}{3} \qquad (eq.6)$$

because of the three-phase equilibrated system we have:

$$\begin{bmatrix} V_{1N} \\ V_{2N} \\ V_{3N} \end{bmatrix} = \frac{1}{3}\cdot \underbrace{\begin{bmatrix} 2 & -1 & -1 \\ -1 & 2 & -1 \\ -1 & -1 & 2 \end{bmatrix}}_{A} \cdot \begin{bmatrix} V_{10} \\ V_{20} \\ V_{30} \end{bmatrix} \qquad (eq.\ 7)$$

The complex form of the motor voltage is given by:

$V_s = V_{sa} + jV_{sb} = \frac{2}{3}\cdot\left[V_{1N} + V_{2N}.a + V_{3N}.a^2\right],\ a = e^{j(2p/3)}$ (*eq.8*).

V_{sa} and V_{sb} are the projections of V_s to an ab fixed 2-axes system (decomposition in a 2-dimensional orthogonal base). V_{1N}, V_{2N}, V_{3N} can be seen as coordinates of $\mathbf{V_s}$ vector in **(1 a a^2)** non-orthogonal base. If we use *eq.8* we obtain constant magnitude transform from tri-phases to bi-phases system. In order to simplify the expression we will speak of **Park "amplitude transform"** or **"amplitude" Park**.

In the same way we can introduce:

$$V_s = V_{sa} + jV_{sb} = \sqrt{\frac{2}{3}}\cdot\left[V_{1N} + V_{2N}.a + V_{3N}.a^2\right], a = e^{j(2p/3)} \qquad (eq.\ 9)$$

which is the **Park "power transform"** (constant power 3? 2 transform) or **"power" Park**.

The 2-levels VSI states can be represented by 8 different configurations. The configuration Sc1=0, Sc2=0, Sc3=0 (000) brings a zero-voltage to the motor (V_s=0). We will note V_s=V0 for this configuration.

From *eq. 2* and *eq. 7* we have $V1(100) = \frac{2}{3}E$ because $V_{1N} = \frac{2}{3}E$, $V_{2N} = -\frac{1}{3}E$, $V_{3N} = -\frac{1}{3}E$. From *eq.8* we can verify the conservation of amplitude in "amplitude" Park:

$$V_s = V_{sa} + jV_{sb} = \frac{2}{3}\,\mathrm{E}\cdot\left[\frac{2}{3} - \frac{1}{3}.a - \frac{1}{3}.a^2\right] = \frac{2}{3}E \qquad (eq.10)$$

So: V_s =V1.

The other configurations are V2(110), V3(010), V4(011), V5(001), V6(101), V7(111). The sequences V0 and V7 are called **zero-voltage sequences** while the others are **active sequences**.

Fig.7 represents these sequences in an ab fixed 2-axes system. These are the only voltages obtainable by a 2-levels VSI. In order to understand the representation of *fig.7* we note that in case of V1(100) from *eq.10* we have: $V_{sa} = \frac{2}{3}E, V_{sb} = 0$ so that coordinates of V1 are ($\frac{2}{3}E$, 0).

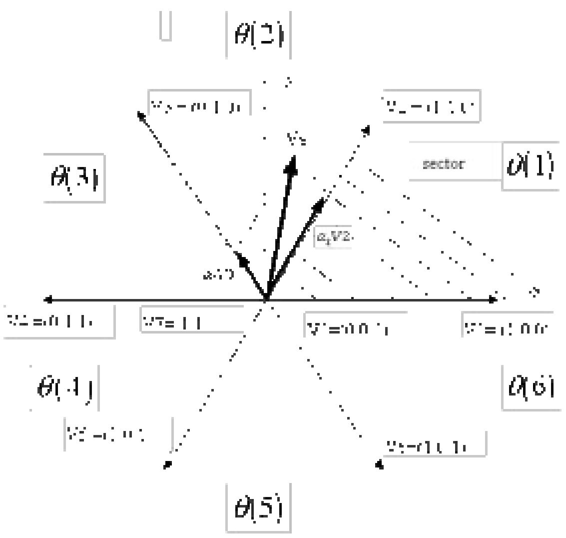

Fig.7 Complex plane representation of 2-levels VSI

It is true that when we are studying the **motor voltages** this representation is sufficient, but if we want to look on the **inverter voltages** (taking into account the zero-voltage) we can see that V7 and V0 are mixed up (origin 0 in *fig.7*). We have to extend the representation to a spatial one in abz coordinates, where V0 and V7 give the direction of z axe (z⊥ ab, $\overline{0z}$ follows $\dot{V7}$) which means we have to use the V_s decomposition in a 3-dimensional orthogonal base.

Consider the space given by an **abc** axes system. *Table 2* gives the coordinates of V_{iN} and V_{i0} in different axes systems we created. *Fig.8* represents the "power" Park voltages (normalised with respect to E) and the two 3-axes systems.

	Sc1	Sc2	Sc3	V_{10} in abc space	V_{20}	V_{30}	V_{1N} in ab plane	V_{2N}	V_{3N}	V_{10} in abz space ("amplitude" Park)	V_{20}	V_{30}	V_{10} in abz space ("power" Park)	V_{20}	V_{30}
V0	0	0	0	$-\frac{E}{2}$	$-\frac{E}{2}$	$-\frac{E}{2}$	0	0	0	0	0	$-\frac{E}{2}$	0	0	$-E\frac{\sqrt{3}}{2}$
V1	1	0	0	$\frac{E}{2}$	$-\frac{E}{2}$	$-\frac{E}{2}$	$\frac{2E}{3}$	$-\frac{E}{3}$	$-\frac{E}{3}$	$\frac{2E}{3}$	0	$-\frac{E}{6}$	$E\sqrt{\frac{2}{3}}$	0	$-E\frac{1}{2\sqrt{3}}$
V2	1	1	0	$\frac{E}{2}$	$\frac{E}{2}$	$-\frac{E}{2}$	$\frac{E}{3}$	$\frac{E}{3}$	$-\frac{2E}{3}$	$\frac{E}{3}$	$\frac{E}{\sqrt{3}}$	$\frac{E}{6}$	$E\frac{1}{\sqrt{6}}$	$E\frac{1}{\sqrt{2}}$	$E\frac{1}{2\sqrt{3}}$
V3	0	1	0	$-\frac{E}{2}$	$\frac{E}{2}$	$-\frac{E}{2}$	$-\frac{E}{3}$	$\frac{2E}{3}$	$-\frac{E}{3}$	$-\frac{E}{3}$	$\frac{E}{\sqrt{3}}$	$-\frac{E}{6}$	$-E\frac{1}{\sqrt{6}}$	$E\frac{1}{\sqrt{2}}$	$-E\frac{1}{2\sqrt{3}}$
V4	0	1	1	$-\frac{E}{2}$	$\frac{E}{2}$	$\frac{E}{2}$	$-\frac{2E}{3}$	$\frac{E}{3}$	$\frac{E}{3}$	$-\frac{2E}{3}$	0	$\frac{E}{6}$	$-E\sqrt{\frac{2}{3}}$	0	$E\frac{1}{2\sqrt{3}}$
V5	0	0	1	$-\frac{E}{2}$	$-\frac{E}{2}$	$\frac{E}{2}$	$-\frac{E}{3}$	$-\frac{E}{3}$	$\frac{2E}{3}$	$-\frac{E}{3}$	$-\frac{E}{\sqrt{3}}$	$-\frac{E}{6}$	$-E\frac{1}{\sqrt{6}}$	$-E\frac{1}{\sqrt{2}}$	$-E\frac{1}{2\sqrt{3}}$
V6	1	0	1	$\frac{E}{2}$	$-\frac{E}{2}$	$\frac{E}{2}$	$\frac{E}{3}$	$-\frac{2E}{3}$	$\frac{E}{3}$	$\frac{E}{3}$	$-\frac{E}{\sqrt{3}}$	$\frac{E}{6}$	$E\frac{1}{\sqrt{6}}$	$-E\frac{1}{\sqrt{2}}$	$E\frac{1}{2\sqrt{3}}$
V7	1	1	1	$\frac{E}{2}$	$\frac{E}{2}$	$\frac{E}{2}$	0	0	0	0	0	$\frac{E}{2}$	0	0	$E\frac{\sqrt{3}}{2}$

Table 2 Space coordinates in abc and abz systems

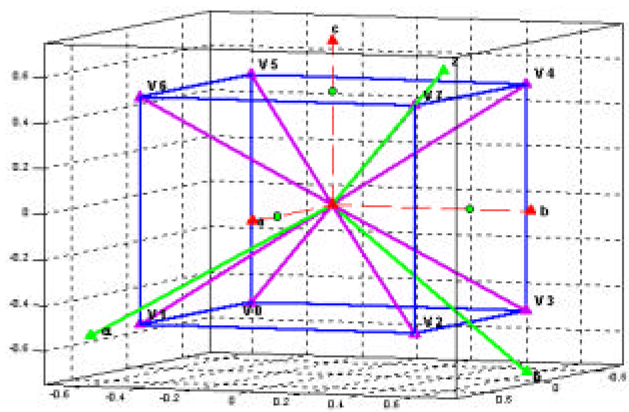

Fig.8 Space representation of "power" Park vectors; available 2-levels inverter voltages

The projections of V0,…V7 vectors in **abc** base are the real values found with *eq. 2* (V_{10} is the **a** axe projection, V_{20} – **b** projection and V_{30} the **c** one). These coordinates can be seen in *Table 2*. As this is what we really obtain with a 2-levels VSI, we will take **ab** plane as the horizontal reference to the graphics. We make the important remark that V0,…V7 point to the vertices of a **cube**. The coordinates of V0,…V7 in abz base using the **Park "power transform"** are the **natural multiplication** of abc coordinates with the axes rotation matrix:

$$X_{\alpha\beta z}=\begin{bmatrix} \sqrt{\frac{2}{3}} & -\frac{1}{\sqrt{6}} & -\frac{1}{\sqrt{6}} \\ 0 & \frac{1}{\sqrt{2}} & -\frac{1}{\sqrt{2}} \\ \frac{1}{\sqrt{3}} & \frac{1}{\sqrt{3}} & \frac{1}{\sqrt{3}} \end{bmatrix} X_{abc} \qquad (eq.\ 11)$$

We can verify it by using for example *eq. 9* in order to obtain V_{sa} and V_{sb} from V_{1N}, V_{2N} and V_{3N}.

We remark that the signification of V0,…V7 is now different in space as in plane: V0,…V7 are in space the real voltages of the inverter (linear combination of V_{i0}), while in a 2-axe representation (*fig.7*) they are positions of V_s motor voltage (*eq. 9*).

It is also interesting to observe Park's "amplitude transform" in our graphical representation; the difference between "power" Park and "amplitude" Park is usually a $\sqrt{2/3}$ coefficient, so that the same matrix as in *eq.11* multiplied by $\sqrt{2/3}$ could give us the $\alpha\beta z$ voltage coordinates for "amplitude" Park. Actually the resulting 0z values do not respect the amplitude conservation principle. This is generally accepted because this form of the matrix is used usually without the third line for a 2-axe representation (motor voltages). In order to conserve the amplitude of the zero-voltage we have to extend Park's transform on the 0z axe using the matrix:

$$\begin{bmatrix} \frac{2}{3} & -\frac{1}{3} & -\frac{1}{3} \\ 0 & \frac{1}{\sqrt{3}} & -\frac{1}{\sqrt{3}} \\ \frac{1}{3} & \frac{1}{3} & \frac{1}{3} \end{bmatrix} \qquad (eq.12)$$

that assures 0z component $V_{N0}=\dfrac{V_{10}+V_{20}+V_{30}}{3}$ to be the **natural** amplitude of the zero-voltage (see *eq.6*).

In fact, the graphical representation of the "amplitude" Park inverter vectors is obtained by rotating the known $\alpha\beta$ coordinates of "amplitude" Park voltages (obtained by *eq. 8*) plus the **z** coordinate obtained as in *eq.6* onto **abc** axes system. This means multiplying the $\alpha\beta z$ coordinates by the inverse of the *eq.11* matrix.

The spatial representation of "amplitude" Park gives a parallelogram included in the "power" Park cube as in *fig.9*.

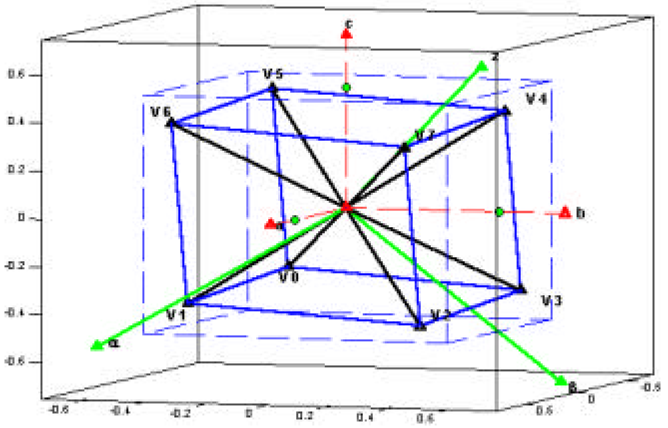

Fig.9 Space representation of "amplitude" Park vectors

This representation cannot be very well exploited; the "power" Park is more suitable for graphical interpretation. On the other hand, "amplitude" Park is more suitable for control drives because using this transform keeps unchanged the amplitude of real values.

If projecting the two parallelograms on the $\alpha\beta$ plane, we can find the representation of *fig.7* with the well-known difference of $\sqrt{2/3}$ between "amplitude" (interior hexagon) and "power" Park (exterior hexagon) (see *fig.10*).

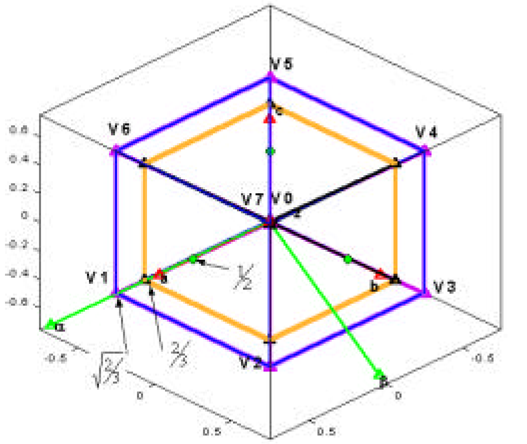

Fig.10 "Amplitude" and "power" Park $\alpha\beta$ plane representations

The $\alpha\beta$ plane projections represent the **motor** line voltages that can naturally be obtained from a 2-levels inverter (V0,…V7). The a, b and c axes projections correspond to the directions of V_{1N}, V_{2N} and V_{3N}. If we want for example to find out the corresponding values of V1 as function of motor line voltages $V_s(V_{1N}, V_{2N}, V_{3N})$=V1, we obtain (2E/3, -E/3, -E/3) by projecting the $\alpha\beta$ coordinates (2/3E,0) or ($\sqrt{2/3}E$,0) on V_{1N}, V_{2N}, V_{3N} plane system: we multiply $\alpha\beta$ coordinates with the inverse of 2x3 Park matrix from *eq.11* or *eq.12* (see also *table 2*).

CLASSIFICATION OF PWM METHODS

In order to explain the necessity of creating other PWM methods we consider the fundamental of the motor line voltage quantified by the **modulation index m_i**. The maximum amplitude of V_{iN} is obtained when applying the **six-step** wave

$$Sci = \begin{cases} 1, \frac{2p}{3}(i-1) \rightarrow \frac{2p}{3}(i-1)+p \ , \\ 0, \text{the rest of the period} \end{cases} \qquad (eq.13)$$

The maximum fundamental value is:

$$V_{six-step} = 2E/p \qquad (eq.14)$$

The modulation index is defined as:

$$m_i = \frac{V_{PWM}}{V_{six\text{-}step}} \qquad (eq.15)$$

The maximum of the **linear** zone is obtained for $V_{PWM} = \frac{1}{2}E$, when $m_i = \frac{(1/2)\cdot E}{2E/p} \cong 0.785$ (zone I, *fig.12*).

We won't include in the following classifications the criterion of the minimum harmonic distortion because generally it is the first criterion to be respected before any other one.

First classification

We will firstly classify the new PWM methods from the complex space representation point of view, where the zero-voltage V_{N0} is the common element.

The main studies developed in PWM literature have been focused on:

- **linearity inverter zone extension**
- **switching losses minimization**
- **acoustical noise diminution**

Almost all new PWM techniques have the same common trace: they are all using in different manners the zero-voltage in order to improve one of the enumerated points. The classification of *fig.11* will be detailed afterwards.

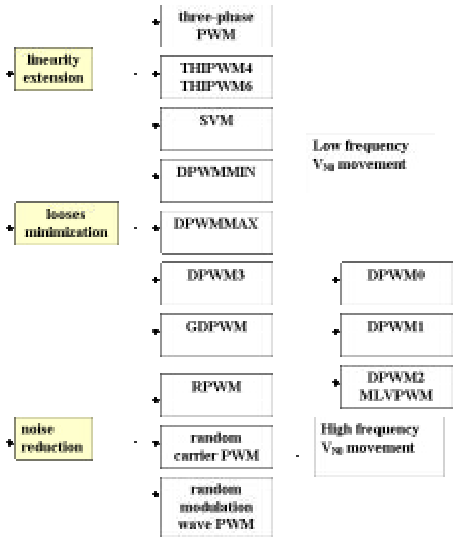

Fig.11 PWM classification function of the zero-voltage movement

The low or high frequency V_{N0} movement means that the average value of V_{N0} changes for smaller or bigger time periods as it will be explained in the followings.

The SPWM principle says that we apply $V_{iref}=V_{iN}$ so that $V_{i0}=V_{iN}$ (average values during a T_e period). This means that what is represented in space is equal to the plane representation; the cube of *fig.8* is flattened to a plan hexagon (the intersection of *a b* plane with the faces of the cube – *fig.12* and *fig.13*). We will detail from the complex cube perspective some of the PWM methods from *fig.11*.

1) THREE-PHASE PWM

The idea of the algebraic **three-phase PWM** [4], [23] was to consider that we have to impose $V_{iref}=V_{i0}$, where V_{i0} is deduced from V_{1N}, V_{2N}, V_{3N}. The motor does not see the inverter V_{i0} voltages. V_{i0} are only a mean, not an aim.

This fact can be considered as a general PWM principle: **as long as we can obtain the expected motor line voltages V_{iN}, we can choose any inverter line voltage we want.**

In fact we can apply to the inverter a reference voltage vector situated at any position in the cube, so that the motor voltages could be situated not only between the limits of the intersection of *a b* plane with the faces of the cube as the SPWM does, but also between the limits of the hexagon created by the projections of the cube to the *a b* plane (*fig.12 and 13*).

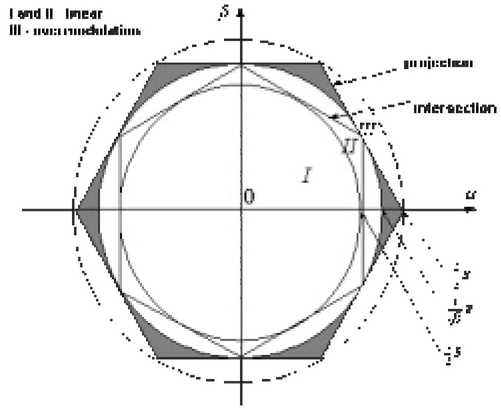

Fig.12 Extension of linearity and over-modulation zones

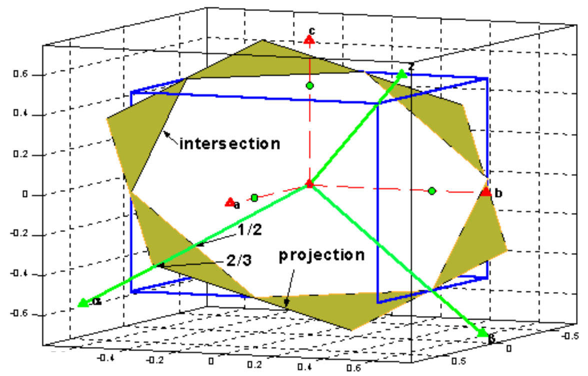

Fig.13 Extension of linearity and over-modulation zones in 3D perspective

Zone I from *fig.12* includes possible trajectories for Vs vectors while using SPWM or regular PWM (linearity limited to m_i=0.785). Zone II represents the second linearity zone (up to m_i=0.907 as we can see further). Zone III represents the overmodulation zone where the trajectory of Vs is not any more a circle (sine wave in time representation); this zone is limited by the projection of the cube on *a b* plane that is the six-step functioning.

As the A matrix from *eq.7* is not invertible, the solution of $V_{i0}=f(V_{iN})$ is not unique. We have to choose particular solutions of this equation. *Fig.14* shows more clearly the idea.

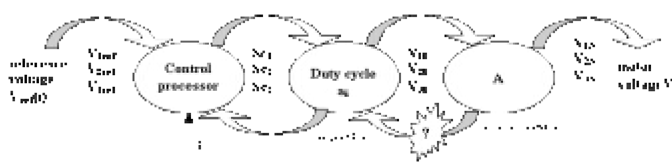

Fig.14 Informational diagram of PWM general principle

We can see that the first part of the diagram represents the SPWM or regular PWM principle: V_{iref} is obtained by imposing V_{i0} (because A^{-1} doesn't exist), while the second part shows that we don't have a return way from V_s to V_{iref} that means that we can impose in different manners the inverter voltages (orders Sc1, Sc2, Sc3) in order to obtain the desired V_{iN}.

In the **SPWM** the $\mathbf{V_{ref}}$ inverter voltage is obtained by applying equal quantities of the V0 and V7 vectors (besides V1,…V6) so that V_{ref} inverter voltage is equal to its *a b* plane projection ($\mathbf{V_s}$ motor voltage).

The infinity of the algebraic PWM solutions proves the possibility to move up or down the **abc** system on Oz axe. This movement deforms the *a b* intersection of the cube from a hexagon to a triangle.

The particular solution chosen for the industrial **three-phase PWM** was to form the zero-voltage from more of V0 than V7 or the other way around. This is a quantity equal to a half of the medium value of the motor line voltages V_{iN} (if $V_{aN} \leq V_{bN} \leq V_{cN}$, a,b,c=1,2,3, $V_{medium}=V_{bN}$). The linearity of the inverter is raised up to $m_i = \frac{p}{2\sqrt{3}} \cong 0.907$. The gain is about 15.47%. *Fig. 15* shows an example: $\mathbf{V_s}$ voltage is obtained by projecting $\mathbf{V_{ref}}$ voltage on $\alpha\beta$ plane. $\mathbf{V_{ref}}$ is displaced from the plane because we apply more of V7 than of V0 in a sampling period.

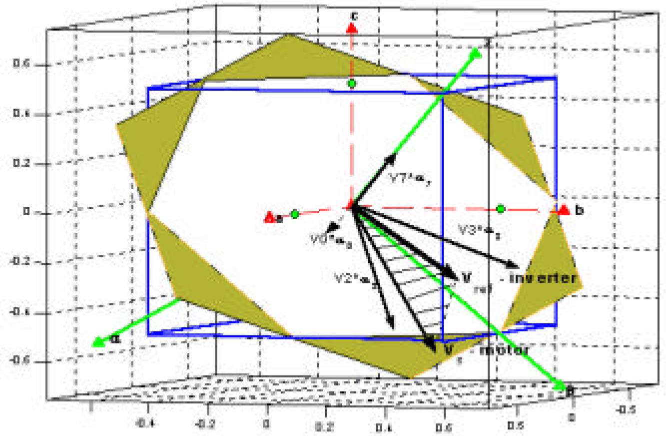

Fig.15 Creation of V_s vector from V0, V7, V2, V3 in three-phase PWM

This technique was in fact preceded by King's analogical realization [5], but its mathematical bases were not evident. We will detail this technique in the next section when showing its complete equivalence with the SVM.

2) THIPWM4 AND THIPWM6

Historically, the three-phase PWM method was preceded by the **THIPWM** methods [3], [6] generally with an analogical practical realization. A part of the 3rd harmonic (1/4 for the THIPWM4 or 1/6 for the THIPWM6) is added to the expected voltages V_{iN} in order to obtain V_{iref}. The result was an increased linearity of the inverter ($m_i = \frac{3\sqrt{3}p}{7\sqrt{7}} \cong 0.881$) reported to the regular PWM and minimum harmonic distortion. Despite this last performance, the complexity of implementing the method (calculating the 3rd harmonic and adding it to non-sinusoidal voltage reference output of regulators) made it an interesting theoretical result, but with poor practical appliance.

As the three-phase PWM or the SVM give almost the same performances as the THIPWM4,6 (better linearity, almost the same harmonic spectrum), their simple implementation made them the most common contemporary PWM.

From a "complex cube" perspective the injection of the 3rd harmonic means the transfer of V_s expected reference vector from the $\alpha\beta$ plane in the upper or in the lower part of the cube (*fig.15*). The $\alpha\beta$ projection of V_s is included in zone II of *fig.12*, but it never reaches the limit hexagon. This means that we don't use the maximum of linear zone.

3) SVM

The SVM (Space Vector Modulation) [2], [7] is the name reserved for the same PWM method as the three-phase PWM, but the pure SVM technique is based on the "space vector" representation of voltages. The original practical implementation uses the **DDT**. There is no comparison modulation wave / carrier neither in theory, nor in practice. By the time of its publication, the principle detailed in the next section has brought a completely different point of view upon the PWM techniques because it has introduced not only a solid theoretical base, but also a new realization (DDT). However we will demonstrate that SVM and three-phase PWM are completely equivalent.

4) DPWM METHODS

The zero-voltage injection has been fully exploited but to different purposes: adding a zero-voltage sequence can serve not only to **linearity extension**, but also to **reducing switching losses** [10], [11], [15], [16], [17], [18]. The third goal is shown at point 5): **noise reduction**.

In order to reduce switching losses the simplest method is not to switch: the idea was possible using zero-voltage sequences that saturate one of the modulation wave of the 3 phases. A lot of methods gathered under the name of DPWM (Discontinuous PWM) have appeared and they differ in the position of saturation level (*fig.16*). We will call **2-phase modulation** the DPWM methods that bring losses reduction.

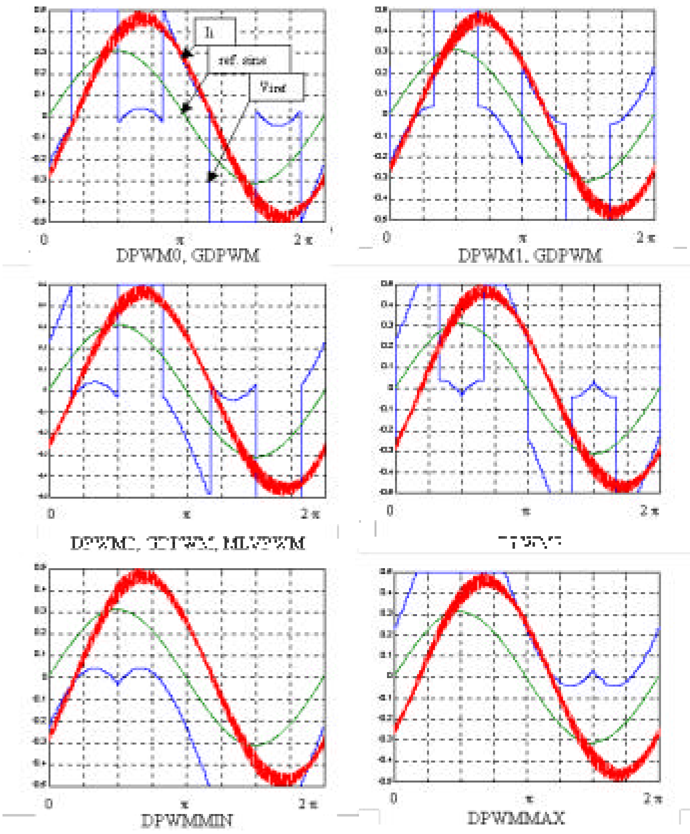

Fig.16 Types of DPWM modulation waves, sinusoidal basic reference and motor current line. Simulation

The basic idea for the 2-phase modulation is to saturate the reference voltage V_{i0} for 1/3 of the 360° period. As every 120° there is a phase with no commutation, the name of 2-phase modulation is justified. *Fig.16* presents the most common DPWM types: the modulation wave is normalised with respect to E, as well as the initial sinusoidal wave; the current is normalised by its maximum. *Fig.16* presents the results of simulations for nominal load point and f_{PWM}=4000 Hz, f_m=25 Hz.

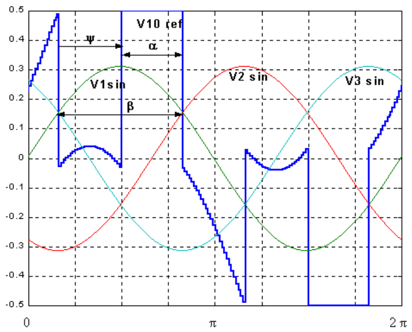

Fig.17 Notations for position of saturation for DPWM techniques

As we can use only a 120° saturation for each phase reference the difference between 2-phase modulation methods consists in choosing the horizon of saturation. **DPWM0, DPWM1, DPWM2** (known also as **MLVPWM**) are particular cases of **GDPWM** (Generalized Discontinuous PWM). As we can see in *Fig.16* the modulation wave is saturated for α =60° every half of the sinusoidal period, but at different angles ψ reported to the initial sinusoidal wave (*fig.17*). ψ =0° for DPWM0, ψ =30° for DPWM1 or ψ =60° for DPWM2. The GDPWM method proposes to modulate the angle ψ function of the current phase reported to the voltage wave. This variation can be made only for ψ =0 to 60°. The basic idea is that the saturation must follow the maximum of the line current so that switchings wouldn't occur by the time the line current is high. This insures a losses reduction up to 50% of SVM or three-phase PWM losses.

These DPWM (DPWM1, DPWM2, DPWM3, GDPWM) modulation waves are obtained from the initial sinusoidal references magnified by

$$V_{NO}=\mathrm{sign}(v_{max})*E/2-v_{max},$$

where v_{max} is the voltage resulted from the maximum magnitude test (absolute maximum of the 3 reference voltages after translation by ?).

The **DPWM3** uses a zero voltage equal to:

$$V_{NO}=\mathrm{sign}(v_{medium})*E/2-v_{medium},$$

where v_{medium} is the intermediate voltage of the 3 references.

The **DPWMMIN** and **DPWMMAX** methods use a zero-voltage signal that is not divided into two 60° fragments (*fig.16*); this brings **a non uniform repartition of Joule losses** on the C1/C4, C2/C5, C3/C6 switches.

The zero-voltage is

$$V_{NO}=-E/2-v_{min},\ \text{for DPWMMIN}$$

$$V_{NO}=E/2-v_{max},\ \text{for DPWMMAX.}$$

All DPWM methods use the maximum of inverter linearity, but losses reduction is different. If compared function of Joule losses on the whole horizon of load variation the best result is obtained with GDPWM, except the zero-load case where the DPWM3 brings the highest reduction of losses.

The reference voltage V_{iref} can be obtained as we have seen by: $V_{iref}=V_{iN}+V_{N0}$, but also by analytical expressions that use the modulation amplitude m_a defined as in (*eq. 4*). For example, the DPWM2 uses:

$$V_{iref}=\frac{E}{2}\begin{cases} 2\cdot m_a\cdot\cos(\alpha-30°)+1, \text{if } 0°\le\alpha<30° \text{ or } 330°\le\alpha<360° \\ 2\cdot m_a\cdot\cos(\alpha+30°)-1, \text{if } 30°\le\alpha<90° \\ 1, \text{if } 90°\le\alpha<150° \\ 2\cdot m_a\cdot\cos(\alpha-30°)-1, \text{if } 150°\le\alpha<210° \\ 2\cdot m_a\cdot\cos(\alpha+30°)+1, \text{if } 210°\le\alpha<270° \\ -1, \text{if } 270°\le\alpha<330° \end{cases}$$

when having the same sine base reference as in *fig.17*.

From a "complex cube" perspective the DPWM methods bring the transfer of V_s expected reference vector from the $\alpha\beta$ plane in the upper on in the lower part of the cube. The $\alpha\beta$ projection of V_s is included in zone II of *fig.12* and it can reach the limit hexagon. While in DPWM0,1,2,3 and GDPWM methods V_s turns from the upper to the lower part of the cube alternatively (in a complete spatial revolution the application time of V0 is the same as V7)(example in *fig.18*), in the DPWMMIN and DPWMMAX methods the average voltage of V_{N0} is not 0, i.e. V_s is **always** in one of the tetrahedrals formed by V0-V1-V2, V0-V2-V3 etc. (*fig.19*) or V7-V1-V2 etc. Remark that these two last methods use only half of the cube.

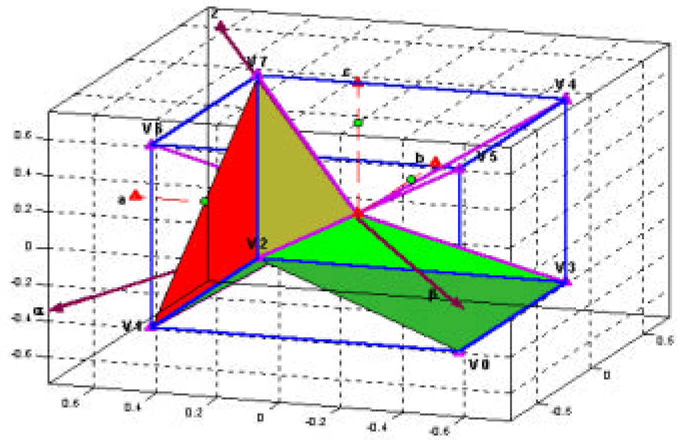

Fig.18 V_{ref} inverter voltage movement for DPWM2 (example for V_s motor voltage in sector $\theta(1)$ and $\theta(2)$, see fig.7)

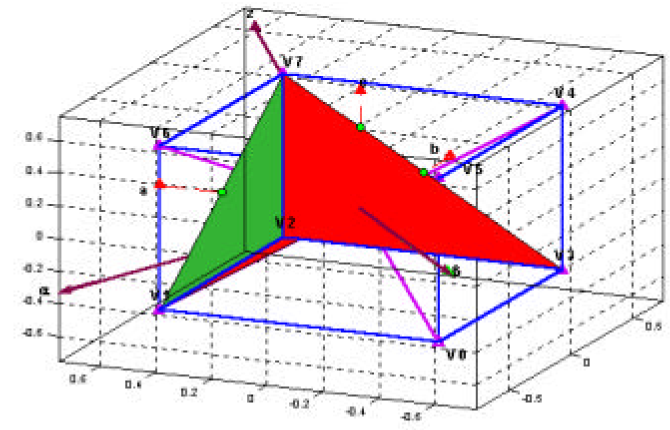

Fig.19 V_{ref} inverter voltage movement for DPWMMAX (example for V_s motor voltage in sector $\theta(1)$ and $\theta(2)$, see fig.7)

5) RANDOM PWM

Other interesting PWM techniques are those used to reduce the acoustical noise of the motor. These techniques are usually based on random modulation. We will show only the 3 most known principles: **random frequency PWM, random carrier PWM** and **random modulation wave PWM**. The first one uses the idea of changing f_{PWM} each sample period. The second one uses random triangle carrier and the third one, a part of the E voltage randomly added or subtracted from the modulation wave as in *fig.20* (both patented by Schneider Electric [21]).

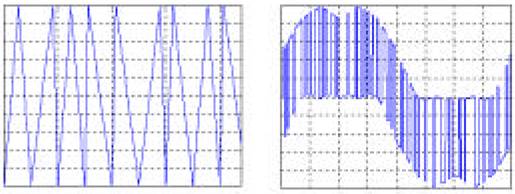

Fig.20 Random carrier and random modulation wave PWM

The result is the same: the spectral energy of the motor line voltage is scattered on a large horizon so that high harmonics around $k*f_{PWM}$ disappear.

We can show an experimental result for the random modulation wave PWM in *fig.21*. The 4 kW ATB motor is not loaded. f_m=25 Hz and f_{PWM}=4000 Hz. The measured V_{21} voltage is applied to the motor using an ATV58 drive. A dSpace card based system is used for measuring and analysis.

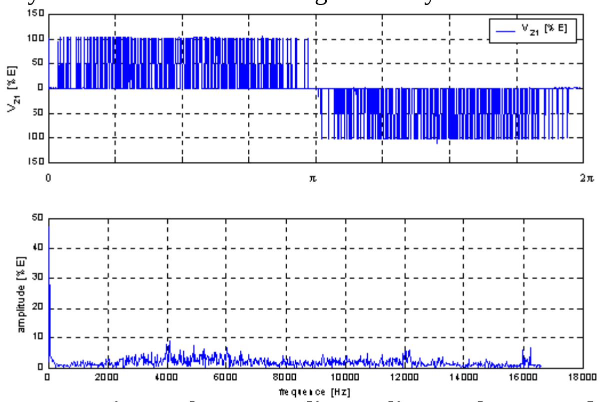

Fig.21 Experimental motor line-to-line voltage and its spectrum for random modulation wave PWM

The random frequency PWM has its DDT equivalent named **RS (Random Switching Frequency),** the random carrier PWM has almost the same principle as the **RCD (Random Displacement of the pulse centre)** and the random modulation PWM is equivalent to the **RZD (Random Distribution of the Zero-voltage vector).** The RZD and the RCD are somehow different from theirs homologues from the modulation wave / carrier technique [24].

We can classify these PWM methods as methods with high frequency V_{N0} movement PWM because V_{ref} voltage change its position from the upper to the lower part of the cube every sampling period T_e.

For the random frequency PWM or the random carrier PWM the zero-voltage is equal to 0 between two sampling instants. For the random modulation wave PWM we have to wait a whole revolution period in order to obtain the average value of V_{N0} equal to 0.

Second classification

A second classification can be made taking into account the practical realization of PWM methods (*fig.22*).

Every regular sampled PWM has its equivalent carrierless realization. For example the well-known three-phase PWM is equivalent to the SVM (see next section).

In order to limit the study we will only name an older PWM technique found in the second classification (the so called **optimized feed forward PWM** [8]). This principle is very useful only when using very low f_{PWM}. It is based on the idea that creating "holes" in the modulated wave at precise positions brings suppression of specific low harmonics.

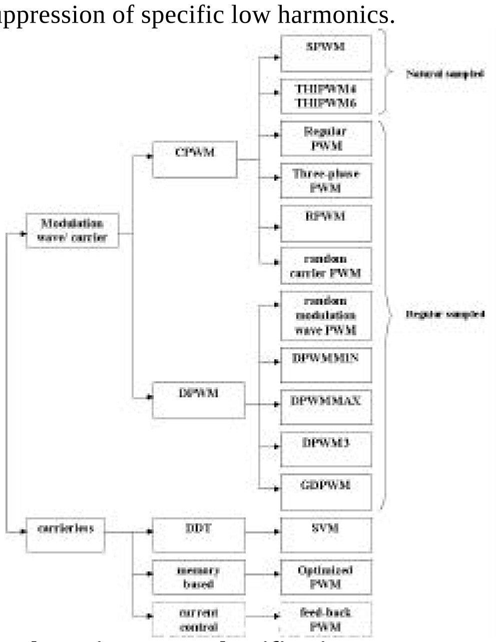

Fig.22 Implantation PWM classification

EQUIVALENCE BETWEEN SVM AND THREE-PHASE PWM

The equivalence between the SVM (DDT implemented) and the three-phase PWM (modulation wave/triangular carrier) means that **the two PWM techniques can be considered as being the same**, because their principles are identical, even if the realization is different. Nevertheless, their importance remains equally shared, because one technique could be more suitable to a particular implantation than the other.

We have to say that what we call nowadays *three-phase PWM* is the PWM technique that has always been implemented using a carrier.

We will firstly give more details on the three-phase PWM by showing that it is superior to any of the THIPWM4, THIPWM6 methods from linearity point of view. The three-phase PWM uses the maximum of the inverter linearity zone. Than, we will explain the realization principle of SVM in order to arrive at the same duty cycles as those of the three-phase PWM.

As we could see in *fig.14* the regular PWM and the SPWM use:

$$V_{iref} = V_{i0} = V_{iN} = V_{max} \cdot \sin(wt + q_i) \qquad (eq.16)$$

$$q_i = -\frac{2p}{3}(i-1) \text{ , i=1,2,3}$$

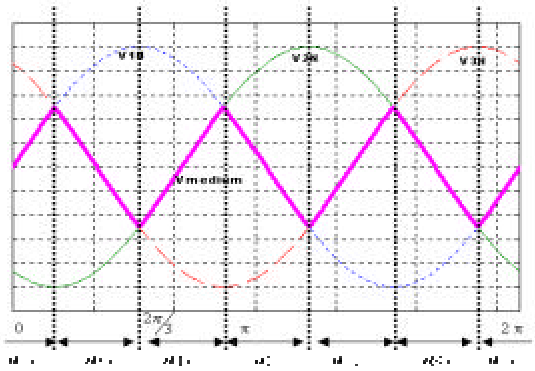

Fig.23

The three-phase PWM uses:

$$V_{iref} = V_{i0} = V_{iN} + V_{NO} = V_{\max} \cdot \sin(wt + q_i) + \frac{V_{medium}}{2}, \qquad (eq.17)$$

The duty cycle from *eq.5* is:

$$a_i = \frac{1}{2} + \frac{V_{iN}}{E}, \text{ for the SPWM} \qquad (eq.18)$$

$$a_i = \frac{1}{2} + \frac{V_{iN}}{E} + \frac{V_{medium}}{2E} \qquad \textbf{(eq.19)}$$

for the three-phase PWM. The zero-voltage is here $V_{medium}/2$.

Firstly, it is simple to prove that adding this quantity represents what we generally call **injection of 3rd harmonic and its multiples**.

We will decompose V_{medium} (*fig.23*) in Fourier series:

$$V_{medium}(t) = A_0 + \sum_{n=1}^{\infty}(A_n \cos nw_3 t + B_n \sin nw_3 t) = \sum_{n=1}^{\infty} B_n \sin 3nwt \qquad (eq.20)$$

$A_0 = 0$ (zero average) and $A_n = 0$ because of the symmetry (when choosing $V_{medium}(t)$ peer function), $w_3 = 3w$ and:

$$B_n = \frac{3V_{\max}}{p} \cdot \frac{1}{9n^2 - 1}\left[\sqrt{3}\sin(np/2) - \sqrt{3}\sin(n\,3p/2) + 2\sin(np)\cos(np)\right] \qquad (eq.21)$$

where n=2k+1, k integer, also because of the symmetries.

As we can see from *eq.20* and *eq.21* V_{medium} is composed by the third harmonic of the motor line voltage and its peer multiples (because of the symmetry).

From *eq.21*: $B_1 = 0.4135\,V_{\max}$, $B_3 = -0.0413\,V_{\max}$, $B_5 = 0.0148V_{\max}$ etc.

$$V_{medium}(t) = B_1 \sin 3wt + B_3 \sin 9wt + B_5 \sin 15wt + ... \qquad (eq.22)$$

The **THIPWM4** and **THIPWM6** methods propose to inject a zero voltage equal to $\frac{V_{\max}}{4}\sin 3wt$ or $\frac{V_{\max}}{6}\sin 3wt$ which are **approximations of $V_{medium}/2$** ($\frac{1}{6} < \frac{B_1}{2} = 0.2067 < \frac{1}{4}$). 1/4 and 1/6 are not the optimum quantities to apply in order to maximise the inverter linearity zone. As the implementation of the three-phase PWM was much simpler, the THIPWM methods have got only little practical signification.

The **SVM** technique proposes a direct calculation of inverter switching times by considering that the expected V_s voltage vector turns in $a\,b$ plane from *fig.7*. In the realization of SVM there is no comparison between a modulation wave and a carrier. As the switching times are directly applied to the inverter, the method was named **DDT**. We will take the example of V_s in sector $q(1)$ (*fig.7*). When V_s is in other sectors the reasoning is similar. V_s is obtained by applying V1, V0, V7, V2 adjacent vectors as in *eq. 23*:

$$\vec{V_S} = a_1 \vec{V1} + a_2 \cdot \vec{V2} + a_0 \cdot \vec{V0} + a_7 \cdot \vec{V7} \qquad (eq.23)$$

a_0, a_1, a_2, a_7 are the application times of each of the V0,V1,V2,V7 vectors as in *fig.24*.

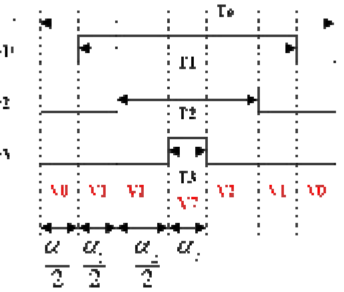

Fig.24 Notations for SVM principle

Let $V1_a$ and $V1_b$ be the projections of V1 on a and b axes of the *fig.7* plane; the same for V2,…V7; we will use the "power" Park conventions for the next equations, but using "amplitude" Park is similar. Only the coefficients differ [7].

The usual implantation of the SVM uses the rotation angle q in order to calculate a_0, a_1, a_2, a_7.

$$a_1 = \frac{|V_s|}{E} \cdot \sqrt{2} \cdot \cos\left(q + \frac{p}{6}\right), a_2 = \frac{|V_s|}{E} \cdot \sqrt{2} \cdot \sin(q),$$

$$a_0 + a_7 = 1 - \frac{|V_s|}{E} \cdot \sqrt{2} \cdot \cos\left(q - \frac{p}{6}\right) \qquad (eq.24)$$

because $a_0 + a_7 + a_1 + a_2 = 1 \qquad (eq.25)$

The a_0, a_1, a_2, a_7 expressions function of a and b projections of voltages are those of *eq. 27*. From *eq. 23* we obtain:

$$\begin{cases} V_{sa} = a_1 V1_a + a_2 V2_a \\ V_{sb} = a_1 V1_b + a_2 V2_b \end{cases} \qquad (eq.26)$$

So that :

$$\begin{cases} a_1 = \frac{1}{E}\left(\sqrt{\frac{3}{2}}V_{sa} - \sqrt{\frac{1}{2}}V_{sb}\right) \\ a_2 = \frac{\sqrt{2}}{E}V_{sb} \\ a_0 = a_7 = \frac{1}{2} - \frac{1}{2E}\left(\sqrt{\frac{3}{2}}V_{sa} + \sqrt{\frac{1}{2}}V_{sb}\right) \end{cases} \qquad (eq.27)$$

In order to solve the equation system formed by *eq.25* and *eq.26* we find the same problem as that of *fig.14*. We have to choose a particular solution in order to find the duty cycles. But we note that the infinity of the existing solutions means the possibility of choosing any V_s position in the cube of *fig.8*. We will show by the following equations that the particular existing solution for the SVM is identical to the three-phase PWM one.

From *eq.27* and *fig.24* we have:

$$\begin{cases} a_1 = a_1 + a_2 + a_7 = \frac{1}{2E}\sqrt{\frac{3}{2}}V_{sa} + \frac{1}{2\sqrt{2}E}V_{sb} + \frac{1}{2} \\ a_2 = a_2 + a_7 = -\frac{1}{2E}\sqrt{\frac{3}{2}}V_{sa} + \frac{3}{2\sqrt{2}E}V_{sb} + \frac{1}{2} \\ a_3 = a_7 = -\frac{1}{2E}\sqrt{\frac{3}{2}}V_{sa} - \frac{1}{2\sqrt{2}E}V_{sb} + \frac{1}{2} \end{cases} \qquad (eq.28)$$

If we apply the 2 to 3 "power" Park transform in *eq.28* we obtain:

$$\begin{cases} a_1 = \frac{1}{E}V_{1N} + \frac{1}{2E}V_{2N} + \frac{1}{2} \\ a_2 = \frac{1}{E}V_{2N} + \frac{1}{2E}V_{2N} + \frac{1}{2} \\ a_3 = \frac{1}{E}V_{3N} + \frac{1}{2E}V_{2N} + \frac{1}{2} \end{cases} \quad (eq.29)$$

In the same manner, in sector $q(2)$ (*fig.7*) we have:

$$\begin{cases} a_1 = \frac{1}{E}V_{1N} + \frac{1}{2E}V_{1N} + \frac{1}{2} \\ a_2 = \frac{1}{E}V_{2N} + \frac{1}{2E}V_{1N} + \frac{1}{2} \\ a_3 = \frac{1}{E}V_{3N} + \frac{1}{2E}V_{1N} + \frac{1}{2} \end{cases} \quad (eq.30)$$

The other sectors give similar equations. *Fig.24* also shows the **time** representation of a complete turn of V_s in the ab complex plan (*fig.7* and *fig.12*). We remark from *fig.23* that V_{2N} for *eq.29* and V_{1N} for *eq.30* are exactly the values of V_{medium} for those sectors so that we can generalise the expressions of the duty cycles:

$$a_i = \frac{1}{2} + \frac{V_{iN}}{E} + \frac{V_{medium}}{2E}$$ **, that is exactly *eq.19*.**

We see by this equivalence that the SVM usually implemented in industry applications is the same as the three-phase PWM.
Other implementations of SVM (as the synchronous time blocked SVM, the so named DI sequence or the DD sequence) [22] can simply be implemented with a modulation wave/carrier technique by using different positions of the triangular carrier or by adding a well define quantity X to the modulation wave reference (this time X was $V_{medium}/2$).

CONCLUSIONS

The goal of this study was to propose graphical analysis tools for PWM techniques. The big variety of PWM existing methods is actually based on the infinity of possibilities for choosing a zero-voltage (V_{N0}) to add to the inverter reference voltages. This idea is mathematically formalised and graphically represented using different decompositions in orthogonal 2D or 3D systems. This synthesis can be a very useful instrument in order to develop or change the PWM techniques on 2-levels VSI.
Three big classes of modulation techniques can be distinguished from the contemporary implemented PWM: methods to extend linearity zone, to minimise switching losses and to reduce acoustical noise. In order to justify this classification the most known PWM are surveyed. It was a good occasion to show that some DPWM can be gathered under the same realization, so that the number of DPWM methods is quite reduced.
Similarly, the PWM techniques can be classified using the practical realization principles: the DDT and the modulation wave / carrier comparison.
The equivalence between the three-phase PWM and the SVM is proved; this shows firstly that the most spread PWM methods of the two techniques of implementation are the same. Secondly, the equivalence is only one example, because the majority of regular sampled PWM could have a DDT realization and vice versa. We could similarly demonstrate it. Nevertheless, one method could be more suited than another to different implementations.

REFERENCES

[1] A. Schönung, H. Stemmler, “Static frequency changers with subharmonic control in conjunction with reversible variable speed AC drives”, Brown Boveri Review, pp. 555-577, Sep. 1964.
[2] H. van der Broeck, H.C. Skudelny, G.V. Stanke, “Analysis and realization of a pulsewidth modulator based on voltage space vectors”, IEEE Transactions on Industry Applications, Vol. 24, No. 1, Jan-Feb. 1988
[3] S.R. Bowes, M.I. Mech, A. Midoun, “Suboptimal switching strategies for microprocessor-controlled PWM inverter drives”, IEE proceedings, Vol. 132, No. 3, pp. 133-148, May 1985
[4] P.F. Seixas, “Commande numérique d’une machine synchrone autopilotée”, PhD rapport, INP Toulouse, 1988
[5] F.G. King, “A three phase transistor class-b inverter with sinewave output and high efficiency”, Inst. Elec. Eng. Conf. Publ. 123, pp.204-209, 1974
[6] G. Buja, G. Indri, “Improvement of pulse width modulation techniques”, Archiv für Elektrotechnik, 57, pp. 281-289, 1975
[7] D. Casadei, G. Serra, A. Tani, L. Zarri, “Analysis of the current ripple in induction motor drives controlled by SVM technique”, EPE, 1999
[8] H.S. Patel, R.G. Hoft, “Generalized techniques of harmonic elimination and voltage control in thyristor inverters: Part I – harmonic elimination”, IEEE Transactions on Industry Applications, vol. IA9, (3), pp. 310-317, 1973
[9] E. Sournac, “Variateur de vitesse pour machine asynchrone”, PhD rapport, INP Toulouse, 1990
[10] A.M. Hava, R.J.Kerman, Th.A. Lipo, “Simple analytical and graphical methods for carrier-based PWM-VSI drives”, IEEE Transactions on Power Electronics, vol.14, No. 1, Jan. 1999
[11] Th.A. Lipo, “A high-performance generalised discontinuous PWM algorithm”, IEEE Transactions on Ind. Appl., Vol. 34, No.5, Sep./Oct. 1998
[12] H. van der Broeck, “Analysis of the voltage harmonics of PWM fed inverters using high switching frequencies and different modulation functions”, ETEP, 1992
[13] J. Holtz, “Pulsewidth Modulation – A survey”, IEEE Trans. on Ind. Electronics, Vol.39, No.5, Oct. 1992
[14] J.T. Boys, P.G. Handley, “Harmonics analysis of space vector modulated PWM waveforms”, IEE Proceedings, Vol.137, Pt. B, No.4, July 1990
[15] D.R. Alexander, S.M. Williams, “An optimal PWM algorithm implementation in a high performance 125 kVA inverter”, IEEE
[16] H. van der Broeck, “Analysis of the harmonics in voltage fed inverter drives caused by PWM schemes with discontinuous switching operation”, EPE, 1991
[17] F. Zare, G. Ledwich, “Space vector modulation technique with reduced switching losses”, EPE, 1999
[18] Trzynadlowski, “Minimum-loss vector PWM strategy for three-phase inverters”, IEEE Trans. on Power Electronics, Vol. 9, No.1, Jan. 1994.
[19] Th.G. Habetler, D.M. Divan, “Acoustic noise reduction in sinusoidal PWM drives using a randomly modulated carrier”, IEEE, pp. 665-671, 1989
[20] S. Hiti, D. Boroyevich, “Small signal modelling of three phase PWM modulators”
[21] Schneider Electric Patent – INPI 94 02428 – “Système de commande d’un onduleur à MLI / US 05552980 –“Inverter control device”

[22] V. Himamshu Prasad, D. Boroyevich, S. Dubovsky, “Comparaison of high frequency PWM algorithms for voltage source inverters”, Virginia Power Electronics
[23] E. Monmasson, J. Faucher, “Projet pédagogique autour de la MLI vectorielle”, 3EI, N°8 – March 1997, pp. 22-36
[24] M.M. Bech, F. Blaabjerg, J.K. Pedersen, “Random modulation techniques with fixed switching frequency for three-phase power converters”, IEEE Transactions on Power Electronics, Vol. 15, No. 4, July 2000

THE AUTHORS

Stefan Laurentiu CAPITANEANU, born in 1976 in Bucharest, received the Diploma Degree in Electrical Engineering from Ecole Nationale Supérieure d’Electrotechnique d’Electronique d’Informatique et d’Hydraulique de Toulouse, France (1999) and the Diploma Degree in Electrical Engineering from the Polytechnic University of Bucharest, Romania (1999).
He is currently preparing a PhD with the Laboratoire d’Electrotechnique et d’Electronique Industrielle, Toulouse, France (UMR INPT-CNRS) and with Schneider Toshiba Inverter Europe, Pacy sur Eure, France. His research deals with PWM optimization.
(tel. 33 6 87 30 68 51, fax. 33 2 32 78 18 89, e-mail Stefan.Capitaneanu@leei.enseeiht.fr)

Bernard de FORNEL was born in 1942 in Bordeaux. He obtained the diploma of engineer from ENSEEIHT in 1965 and the Doctorat es Sciences in 1976. He is full professor (1980) at Institut National Polytechnique of Toulouse. His teaching and research fields are in the control of electrical drives.
He is responsible for the Doctorat formation in Electrical Engineering, member of several ISC of international Conferences. He has published more than 150 international publications and directed more than 50 PhDs.
(tel. 33 5 61 58 82 55, fax. 33 5 61 63 88 95, e-mail Bernard.de.Fornel@leei.enseeiht.fr)

Maurice FADEL received the PhD. degree in electrical engineering from the Institut National Polytechnique de Toulouse in 1988 (France). He works in the control of electrical systems group of the Laboratoire d’Electrotechnique et d’Electronique Industrielle (LEEI, UMR INPT- CNRS) since 1985.
He is currently Professor in the Ecole Nationale Supérieure d’Electronique, d’Electrotechnique, d’Informatique, d’Hydraulique et des Télécommunications de Toulouse, his teaching covers control theory and design of control laws in electrical systems (static converter and electrical machine). Since 1998, he is the leader of the Control of Electrical Systems group. His owns researches concerns modelisation and control of static converters, power electronics machines and drives.
(tel. 33 5 61 58 83 36, fax. 33 5 61 63 88 95, e-mail Maurice.Fadel@leei.enseeiht.fr)

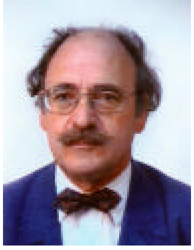

Jean FAUCHER
French; age: 58
Electrical Engineer from Toulouse INP (Institut National Polytechnique) in 1967
1st thesis (docteur-ingénieur) in 1969
2nd thesis (docteur ès Sciences) in 1981 from INP Toulouse on "reluctance machines"
University Professor since 1985 teaching Automatic Control and Electrical Engineering at INPT.
He is researcher with CNRS Laboratory: LEEI (Laboratoire d'Electrotechnique et d'Electronique Industrielle). His main field of interest concern modelling of electrical machines and converters for automatic control of machine converter drives.
(tel. 33 5 61 58 83 54, fax. 33 5 61 63 88 95, e-mail Jean.Faucher@leei.enseeiht.fr)

Antonio ALMEIDA is graduated in Electrical Engineering from Ecole Nationale Supérieure de l’Electronique et de ses Applications (ENSEA), Cergy-Pontoise, France, in 1985. He received the Diploma Degree in Electrical Engineering from Université Pierre et Marie Curie, Paris 6, France, in 1992.
He is working as a research and development engineer with Schneider Toshiba Inverters Europe (STIE), Paçy-sur-Eure, France. His fields of interest are variable speed drives, motor control and power electronics.
(tel. 33 2 32 78 18 68, fax. 33 2 78 18 89, e-mail: antonio_almeida@mail.schneider.fr)